

MerA functions as a hypothiocyanous acid reductase and defense mechanism in *Staphylococcus aureus*

Heather L. Shearer¹ | Vu V. Loi² | Paul Weiland^{3,4} | Gert Bange^{3,5} | Florian Altegoer^{3,6} | Mark B. Hampton¹ | Haike Antelmann² | Nina Dickerhof¹

¹Centre for Free Radical Research, Department of Pathology and Biomedical Science, University of Otago Christchurch, Christchurch, New Zealand

²Freie Universität Berlin, Institute of Biology-Microbiology, Berlin, Germany

³Center for Synthetic Microbiology (SYNMIKRO), Department of Chemistry, Philipps-University Marburg, Marburg, Germany

⁴Center for Tumor Biology and Immunology, Department of Medicine, Philipps-University Marburg, Marburg, Germany

⁵Max-Planck Institute for Terrestrial Microbiology, Marburg, Germany

⁶Institute of Microbiology, Heinrich Heine University Düsseldorf, Düsseldorf, Germany

Correspondence

Nina Dickerhof, Centre for Free Radical Research, University of Otago Christchurch, P.O. Box 4345, Christchurch 8140, New Zealand.
Email: nina.dickerhof@otago.ac.nz

Funding information

Canterbury Medical Research Foundation, Grant/Award Number: 05/20; University of Otago Research, Grant/Award Number: 3579; Sir Charles Hercus Health Research Fellowship; Health Research Council of New Zealand; Deutsche Forschungsgemeinschaft, Grant/Award Number: 2573, AN746/4-2 and AN746/4-1

Abstract

The major pathogen *Staphylococcus aureus* has to cope with host-derived oxidative stress to cause infections in humans. Here, we report that *S. aureus* tolerates high concentrations of hypothiocyanous acid (HOSCN), a key antimicrobial oxidant produced in the respiratory tract. We discovered that the flavoprotein disulfide reductase (FDR) MerA protects *S. aureus* from this oxidant by functioning as a HOSCN reductase, with its deletion sensitizing bacteria to HOSCN. Crystal structures of homodimeric MerA (2.4 Å) with a Cys₄₃-Cys₄₈ intramolecular disulfide, and reduced MerACys₄₃S (1.6 Å) showed the FAD cofactor close to the active site, supporting that MerA functions as a group I FDR. MerA is controlled by the redox-sensitive repressor HypR, which we show to be oxidized to intermolecular disulfides under HOSCN stress, resulting in its inactivation and derepression of *merA* transcription to promote HOSCN tolerance. Our study highlights the HOSCN tolerance of *S. aureus* and characterizes the structure and function of MerA as a major HOSCN defense mechanism. Crippling the capacity to respond to HOSCN may be a novel strategy for treating *S. aureus* infections.

KEYWORDS

Heme peroxidase, HypR, MRSA, RclA, SPD_1415

Heather L. Shearer and Vu V. Loi contributed equally to this work.

This is an open access article under the terms of the [Creative Commons Attribution-NonCommercial-NoDerivs](https://creativecommons.org/licenses/by-nc-nd/4.0/) License, which permits use and distribution in any medium, provided the original work is properly cited, the use is non-commercial and no modifications or adaptations are made.

© 2023 The Authors. *Molecular Microbiology* published by John Wiley & Sons Ltd.

1 | INTRODUCTION

Staphylococcus aureus is a common commensal bacterium that asymptotically colonizes the anterior nares and the skin in up to 30% of the healthy human population. *S. aureus* can also cause life-threatening infections, such as bacteremia and pneumonia, especially in immunocompromised patients (Laux et al., 2019; Sakr et al., 2018). Multi-drug resistant strains, particularly methicillin-resistant *S. aureus* (MRSA) isolates, are prevalent in the hospital and the community, posing a significant risk to human health (Vestergaard et al., 2019). Understanding how *S. aureus* is capable of evading host immune defenses might hold the key to uncovering new treatment strategies against MRSA infections.

Staphylococcus aureus is highly adapted to its host and has evolved many strategies to survive the onslaught of the immune system. These include the synthesis and secretion of virulence factors to avoid opsonization and neutrophil phagocytosis, disrupt host tissue integrity, or inhibit host proteases, allowing them to disseminate through the body and escape from the immune system (de Jong et al., 2019; Pietrocola et al., 2017). Even once phagocytosed by neutrophils, *S. aureus* can resist both oxygen-dependent and -independent killing mechanisms (de Jong et al., 2019). Oxygen-dependent killing is based on the NADPH-oxidase-mediated production of superoxide, which myeloperoxidase (MPO) converts to hydrogen peroxide (H_2O_2) and subsequently to the potent bactericidal hypochlorous acid (HOCl) (Hampton et al., 1998; Harrison & Schultz, 1976; Winterbourn et al., 2006). To cope with neutrophil-derived oxidants, *S. aureus* produces small molecules that act as antioxidants (bacillithiol, staphyloxanthin) or inhibitors of MPO (staphylococcal peroxidase inhibitor), and enzymes that degrade oxidants (superoxide dismutase, catalase, peroxiredoxins) or repair the resulting damage (thiol-disulfide oxidoreductases) (de Jong et al., 2017; Loi et al., 2018a; Mandell, 1975; Posada et al., 2014). In addition, redox-sensitive transcription factors in *S. aureus* sense and respond to neutrophil oxidants to regulate the expression of these defense mechanisms in response to HOCl (HypR) and H_2O_2 (PerR) (Horsburgh et al., 2001; Linzner et al., 2021; Loi et al., 2018a).

While the HOCl-defense mechanisms of *S. aureus* have been explored (Linzner et al., 2021), there are only a few studies that have examined the response of *S. aureus* to hypothiocyanous acid (HOSCN), a front-line oxidant produced in secretory fluids. HOSCN is generated by host heme peroxidases, using H_2O_2 from sources such as epithelial cell dual oxidase (DUOX) (van der Vliet, 2008), to oxidize thiocyanate (SCN^-) at sites of *S. aureus* colonization and infection, including the nasopharynx and the lung. Under physiological conditions, the main peroxidase enzyme generating HOSCN is lactoperoxidase (LPO), which is secreted into the airway mucosa (Wijkstrom-Frei et al., 2003). Eosinophil peroxidase (EPO) and the neutrophil enzyme myeloperoxidase (MPO) will also contribute to HOSCN production under inflammatory conditions (van Dalen et al., 1997; van Dalen & Kettle, 2001). Because chloride concentrations typically exceed those of SCN^- , HOCl is considered the chief oxidant produced by MPO activity in plasma and inside neutrophil

phagosomes, even though SCN^- is the preferred substrate for this enzyme (van Dalen et al., 1997). However, the concentration of SCN^- can reach 650 and 800 μM in the lung and nasal airway fluid, respectively (Lorentzen et al., 2011; Wijkstrom-Frei et al., 2003), making HOSCN the predominant product of peroxidase activity at these sites. While HOCl is a promiscuous oxidant, HOSCN is specific for thiol groups (Pattison & Davies, 2006; Skaff et al., 2009), and is known to inhibit thiol-dependent proteins involved in metabolism and substrate transport in bacteria (Carlsson et al., 1983; Oram & Reiter, 1966; Shin et al., 2001; Thomas & Aune, 1978).

The ability of *S. aureus* to successfully colonize and infect at sites of high HOSCN production points to an inherent HOSCN tolerance of these bacteria. However, relatively little is known about how *S. aureus* defends against HOSCN stress. In 2019, Day et al. found that some clinical MRSA isolates survive much higher concentrations of HOSCN generated by a LPO/ SCN^- system than *Pseudomonas aeruginosa* isolates (Day et al., 2020). Similarly, we found that another Gram-positive mucosae commensal and lung pathogen *Streptococcus pneumoniae* survived HOSCN significantly better than *P. aeruginosa* (Shearer et al., 2022a). Since both *S. pneumoniae* and *S. aureus* colonize and cause serious infections in HOSCN-generating niches, they may have evolved unique HOSCN defense mechanisms that underlie their HOSCN tolerance. We recently identified a flavoprotein disulfide reductase (FDR) enzyme in *S. pneumoniae* that uses NAD(P)H to reduce HOSCN and contributes to protection against this oxidant (Shearer et al., 2022b). We named this pneumococcal enzyme hypothiocyanous acid reductase (Har). Furthermore, the *Escherichia coli* enzyme RclA, a homolog of Har, has been reported to function as a HOSCN reductase and protective mechanism in *E. coli* (Meredith et al., 2022). In this study, we investigated the expression, regulation, function, and structure of the homologous FDR enzyme MerA of *S. aureus* and demonstrated its role in the defense against HOSCN.

2 | RESULTS

2.1 | *Staphylococcus aureus* tolerates HOSCN better than other bacteria

To determine the relative HOSCN tolerance of *S. aureus* compared with other respiratory tract pathogens, we conducted HOSCN killing assays (Figure 1a,b). We have previously reported that *P. aeruginosa* are killed after 30 min of exposure to a high dose of 800 μM HOSCN (Shearer et al., 2022a), whereas killing of *S. pneumoniae* was only observed after 3 h (Shearer et al., 2022c). Here, we found that the *S. aureus* USA300 clinical isolate can survive high doses of HOSCN for >3 h (Figure 1a). To directly compare the relative HOSCN sensitivity of these bacteria, we performed dose-response experiments (Figure 1b). While only 100 μM of HOSCN was required to completely kill *P. aeruginosa* after 3 h, 400 μM was needed for *S. pneumoniae* (Figure 1b). In contrast, the viability of *S. aureus* was not substantially impacted even when treated with the highest dose of 800 μM (Figure 1b). Collectively our data highlights the remarkable HOSCN tolerance of *S. aureus*.

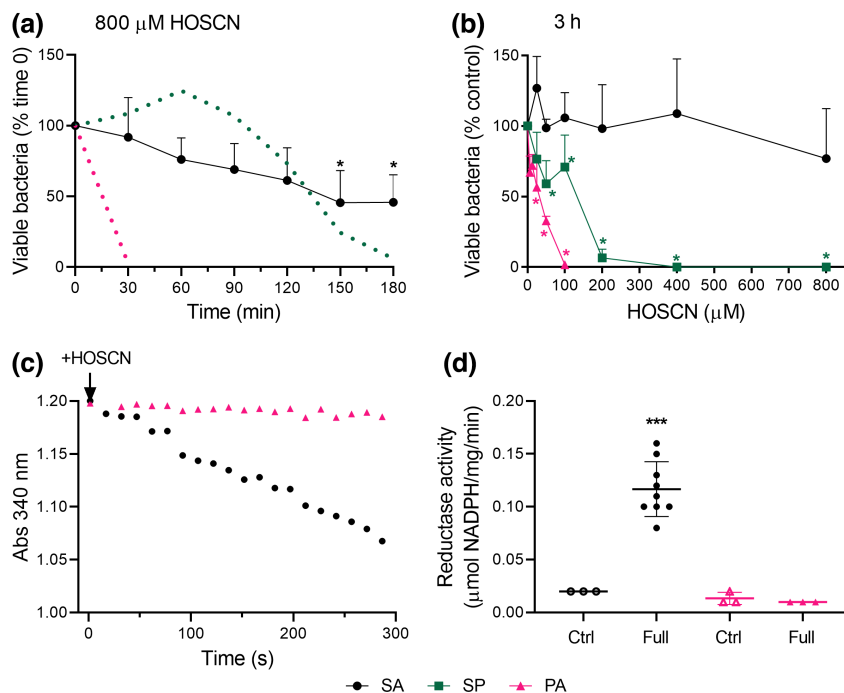


FIGURE 1 Sensitivity of different bacterial species to HOSCN and HOSCN reductase activity in bacterial lysates. (a, b) *Staphylococcus aureus* USA300 (SA, black circles), *Streptococcus pneumoniae* D39 (SP, green squares) and *Pseudomonas aeruginosa* PAO1 (PA, pink triangles) were treated at 2.5×10^5 CFU/ml with (a) 800 μ M HOSCN at 37°C for up to 3 h or (b) with increasing concentrations of HOSCN for 3 h. Viable bacteria were determined by plate counts and expressed relative to those at t_0 in (a) and to the untreated (0 μ M HOSCN) control at the 3 h time point in (b). The viability of untreated *S. aureus* at 180 min was not significantly different to t_0 , that is, 95 ± 10 (mean \pm SD). Time course survival data for SP and PA were already published in (Shearer et al., 2022a; Shearer et al., 2022c) and are shown as dotted lines in (a) for comparison. Symbols represent means \pm SD of at least three independent experiments. A significant difference from the 100% control, that is, viable bacteria at t_0 in (a) and untreated bacteria at 3 h in (b), was determined by one-way ANOVA with Dunnett's multiple comparison test and is indicated with * $p < 0.05$. (c) Consumption of NADPH (200 μ M) by bacterial lysates was measured in 100 mM phosphate pH 7.4, 1 mM EDTA by monitoring the loss of absorbance at 340 nm for 5 min following the addition of 100 μ M HOSCN. For clarity, the starting OD for all traces was set to 1.2. This is a representative trace of ≥ 3 independent experiments. (d) Reductase activity in bacterial lysates after addition of 100 μ M HOSCN (Full system, Full; closed symbols) or buffer (Control, Ctrl; open symbols) to bacterial lysates was expressed as the amount of NADPH consumed ($\Delta A / (6220 / (M \times cm) \times 1 \text{ cm})$) per min relative to the protein content as determined by Bradford. Each symbol represents an independent experiment. A significant difference between NADPH consumption in the absence and presence of HOSCN for each bacterial strain was determined by unpaired, two-tailed t test and is indicated with *** $p < 0.001$.

To determine whether a HOSCN reductase might be contributing to the tolerance of *S. aureus*, similar to what we recently reported for *S. pneumoniae* (Shearer et al., 2022b), we assessed NADPH consumption in bacterial lysates exposed to HOSCN (Figure 1c,d). While *P. aeruginosa* lysates had no HOSCN reductase activity, we observed similar levels of reductase activity in lysates of *S. aureus* ($0.11 \pm 0.03 \mu\text{M NADPH/mg/min}$, mean \pm SD) to what we had previously measured in *S. pneumoniae* ($0.08 \pm 0.02 \mu\text{M NADPH/mg/min}$, mean \pm SD) (Shearer et al., 2022b). These results indicate that *S. aureus*, like *S. pneumoniae*, possesses a HOSCN reductase enzyme.

2.2 | The structure of *S. aureus* MerA supports its function as a HOSCN reductase

Sequence alignments revealed that the *S. aureus* FDR MerA is a close homolog of the recently characterized HOSCN reductases

Har/SPD_1415 in *S. pneumoniae* (50% identities and 66% positives) and RclA in *E. coli* (50% sequence identity, 65% positives) (Figure S1) (Derke et al., 2020; Loi et al., 2018a; Meredith et al., 2022). These enzymes belong to the group I FDR family, dimeric proteins that transfer reducing equivalents from NAD(P)H to a bound FAD co-factor and subsequently to a redox-active disulfide, which in its dithiol state can interact with the substrate to reduce it (Argyrou & Blanchard, 2004).

We solved the crystal structures of MerAC₄₃S and MerA at a resolution of 1.6 and 2.4 Å, respectively (Table S1). The N-terminal cysteine of the catalytic CXXXXC motif, C₄₃, was replaced in MerAC₄₃S to trap MerA in its reduced conformation. Both proteins were present as homodimers in the asymmetric unit with the two protomers (Figure 2a,b and Figure 3a–c). The structures revealed the characteristic group I FDR family domains: the N-terminal FAD-binding domain with the conserved C₄₃X₄₄X₄₅X₄₆C₄₈ redox-active site, the NADPH-binding domain, the central domain and the C-terminal dimer interface domain with the conserved H₄₂₇X₄₂₈X₄₂₉X₄₃₀E₄₃₂ motif

(Argyrou & Blanchard, 2004; Baek et al., 2020) (Figure 2a,b). In the MerA structure, Cys₄₃ and Cys₄₈ were oxidized to an intramolecular disulfide (Figure 3c,f). The FAD cofactor was bound in close proximity to the C/S₄₃XXXXC₄₈ active site motif in each subunit of both the MerAC₄₃S and MerA dimers (Figure 2a,b and Figure 3a–c). Helices α 2, α 3, and α 4 (aa 36–81) could not be resolved in one subunit of the MerA structure due to poor resolution in this region. The enlarged view into the MerAC₄₃S active site revealed that the distance of C₄₈ to C₄₃S and the C4a atom of the isoalloxazine ring of FAD was 3.6 and 3.8 Å, respectively, consistent with its ability to form a redox-active disulfide and to interact with the cofactor (Figure 2c). An overlay of the MerAC₄₃S and MerA structures showed no major structural differences between the two active sites (Figure 3d–f).

The MerA active site superimposes well onto that of the HOSCN reductase RclA (Baek et al., 2020; Meredith et al., 2022), with a root mean square deviation of 1.2 Å across 754 C α atoms (Figures S1 and S2), suggesting that MerA, like RclA, has the capacity to reduce HOSCN.

2.3 | HOSCN reductase activity in *S. aureus* is associated with MerA expression and is elevated following HOSCN stress

To demonstrate that the observed HOSCN reductase activity in *S. aureus* lysates is facilitated by MerA, we used *S. aureus* USA300JE2 strains. Lysates from a $\Delta merA$ mutant, unlike those from wild-type (WT) bacteria, showed no significant increase in NADPH consumption when HOSCN was added compared with background (Figure 4a). In lysates from a *merA*⁺ complemented strain, which constitutively expresses *merA* ectopically from the plasmid pRB473 in the presence of 1% xylose (Loi et al., 2018a), HOSCN reductase activity was found to be 1000-fold higher than in the WT strain (Figure 4a). In contrast, complementation with the empty pRB473 plasmid (data not shown) or the *merAC*₄₃S allele (Figure 4a) did not restore HOSCN activity in the $\Delta merA$ mutant, demonstrating that the N-terminal cysteine of MerA's CXXXXC motif is required for activity.

Transcription of *merA* in *S. aureus* is known to be regulated by the redox-sensitive repressor HypR (Loi et al., 2018a). Constitutive

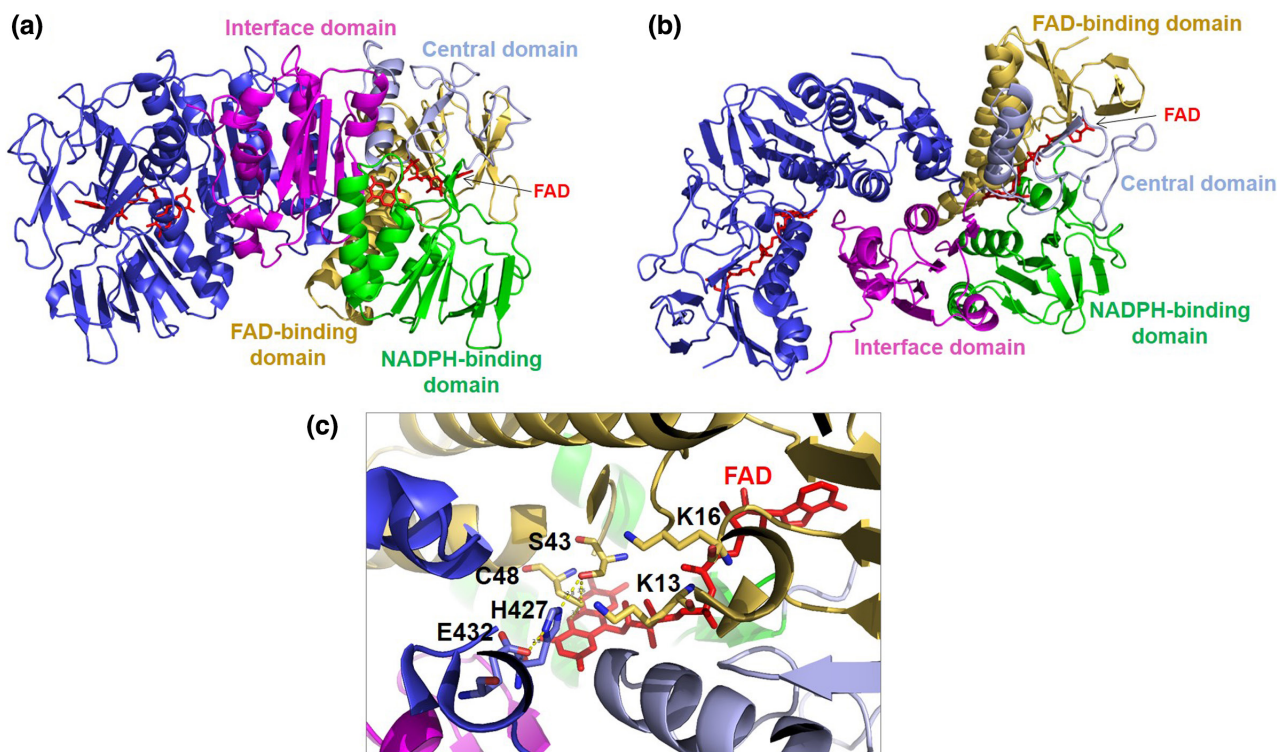


FIGURE 2 Crystal structure of MerAC₄₃S and close-up of the active site. (a, b) Overall assembly of the MerAC₄₃S dimer (PDB 8AJK) in front (a) and top view (b). One subunit of the dimer is in blue, the other subunit is color-coded based on the four MerA domains: The N-terminal FAD-binding domain with the C₄₃SXXXXC₄₈ active site motif (gold), the NADPH-binding domain (green), the central domain (light blue) and the interface domain with the conserved H₄₂₇PTMAE₄₃₂ motif (magenta). The protein structures are presented as ribbon and the FAD cofactors in each subunit as red sticks. (c) Close-up of the C₄₃SXXXXC₄₈ active site motif and the bound FAD cofactor in the MerAC₄₃S structure. The FAD cofactor is shown as red sticks and the important residues K₁₃, K₁₆, C₄₃S, C₄₈, H₄₂₇, and E₄₃₂ are also presented as sticks in the ribbon structure. Atoms of the amino acid sticks are colored by element: sulfur (yellow), oxygen (red), and nitrogen (blue). The dotted yellow lines indicate the distance between the interacting residues C₄₃S and C₄₈ in one subunit (3.6 Å), the H₄₂₇ and E₄₃₂ in the opposing subunit (2.8 Å), of C₄₈ with the C4a atom of the FAD cofactor (3.8 Å), and of C₄₃S with H₄₂₇ (2.8 Å).

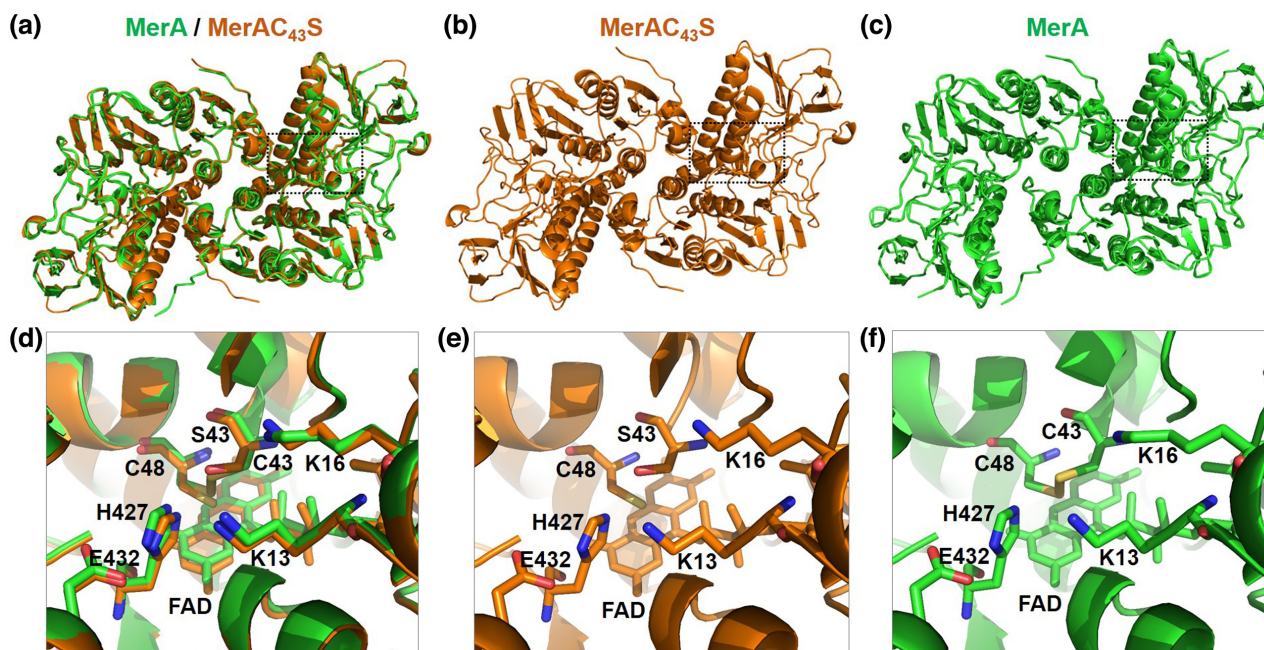


FIGURE 3 Overlay of the oxidized MerA disulfide and the MerAC₄₃S structures with a close-up of both active sites. (a–c) The overlaid and individual structures of MerA (PDB 8AJJ green) and MerAC₄₃S (PDB 8AJK, orange) are shown in top view as ribbon presentations. (d–f) Close-up views of the active sites from the top view of the structures from (a–c), respectively. The FAD cofactors and the critical interacting residues K₁₃, K₁₆, C₄₃/C₄₃S, C₄₈, H₄₂₇, and E₄₃₂ are presented as sticks in the close-up views. Atoms of the amino acid sticks are colored by element: sulfur (yellow), oxygen (red), and nitrogen (blue).

transcription of *merA* in a Δ *hypR* mutant was mirrored by a 100-fold increase of HOSCN reductase activity compared with WT (Figure 4a). Complementation of the Δ *hypR* mutant with *hypR* expressed from plasmid pRB473 (*hypR*⁺, Figure 4a), but not the empty plasmid (data not shown), decreased reductase activity below the levels observed in WT lysates due to overexpression of HypR.

The HypR repressor has been shown to be inactivated in *S. aureus* under HOCl stress due to thiol-oxidation, resulting in derepression of *merA* transcription (Loi et al., 2018a). As such, we investigated whether HOSCN reductase activity is increased in WT cells following HOSCN stress. Indeed, HOSCN reductase activity was significantly higher in exponentially growing WT bacteria after 60 min exposure to 100 μ M HOSCN compared with the untreated control (Figure 4b). This was not observed in the Δ *merA* mutant demonstrating that the increased activity of WT cells in response to HOSCN stress can be attributed to MerA.

To investigate whether MerA activity was associated with bacterial consumption of HOSCN, we measured the decline of extracellular HOSCN when added to intact *S. aureus* cells (Figure 4c,d). Addition of 200 μ M HOSCN to WT cells resulted in slightly accelerated HOSCN consumption compared with media alone (Figure 4c), but this was only statistically significant in WT complemented with empty plasmid where experiments were performed in xylose/chloramphenicol-containing media (Figure 4d). We did not detect a difference in HOSCN decline in the presence of the Δ *merA* mutant or the *hypR*⁺ and *merAC*₄₃S complemented strains. In contrast, the high HOSCN reductase activity in the Δ *hypR* and *merA*⁺ strains significantly decreased the amount of extracellular HOSCN (Figure 4c,d).

The Δ *merA* and Δ *hypR* strains complemented with empty plasmids consumed HOSCN similarly to their corresponding mutant strains (data not shown).

Together, these results show that the *S. aureus* MerA FDR enzyme functions as a HOSCN reductase, which is elevated under HOSCN stress.

2.4 | Transcription of *merA* is induced under HOSCN stress

To confirm that the increase in reductase activity in response to HOSCN is regulated at a transcriptional level, we used Northern blot analyses. We found that the transcription of *merA* was repressed in the *S. aureus* USA300JE2 WT strain both during exponential growth and in stationary phase (Figure 5a). Exposure of WT cells to 100 μ M HOSCN for 30 min during exponential growth resulted in the strong upregulation of transcription of the bicistronic *hypR-merA* operon (Figure 5a). Transcription of the 1.8 kb *hypR-merA* operon in WT cells after HOSCN stress was induced to a similar level as observed for the 1.5 kb *merA* transcript in the untreated Δ *hypR* mutant, in which *merA* transcription is fully derepressed (Figure 5a) (Loi et al., 2018a). The absence of the *merA* transcript in the Δ *merA* mutant confirmed the clean deletion of this gene. Expression of the 1.5 kb transcript of *merA* was fully restored in the *merA*⁺ complemented strain to the same level as observed in the Δ *hypR* mutant (Figure 5a). Together, these data indicate that HOSCN exposure leads to HypR-regulated derepression of *merA* transcription in *S. aureus*.

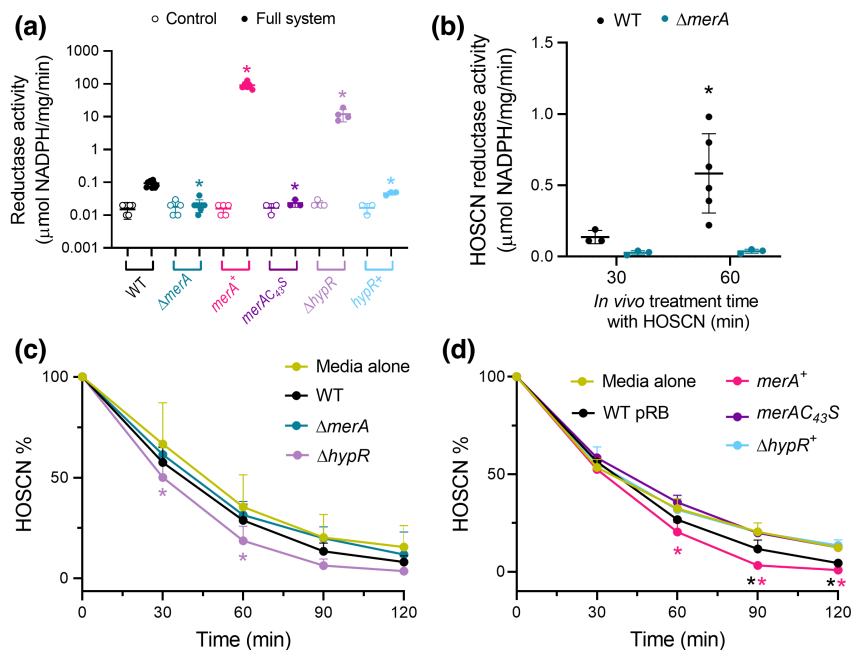


FIGURE 4 HOSCN reductase activity in *Staphylococcus aureus* lysates is mediated by MerA. (a) Reductase activity was measured in lysates of overnight cultures of *S. aureus* USA300JE2 WT, $\Delta merA$ and $\Delta hypR$ mutants and the $merA^+$, $merAC_{42}S$, and $hypR^+$ complemented strains by measuring the consumption of NADPH after the addition of 100 μ M HOSCN (Full system, closed symbols) or buffer (Control, open symbols) to the lysate as described in Figure 1. Each symbol represents a separate experiment using lysates obtained from independent cultures and the bar is the mean \pm SD. A significant difference between the activity measured in the full system for each strain compared with the full system containing WT lysates was determined by one-way ANOVA with Dunnett's multiple comparison test using the log-transformed data and is indicated by * $p < 0.01$. (b) Exponentially growing *S. aureus* USA300JE2 WT and $\Delta merA$ mutant cultures were incubated with 100 μ M HOSCN for 30 or 60 min, then washed and lysed. Reductase activity in bacterial lysates was measured in the full system as described in (a). A significant difference compared with the HOSCN reductase activity measured in cells incubated with buffer instead of HOSCN was determined by unpaired t test and is indicated by * $p < 0.05$. (c), (d) Exponentially growing *S. aureus* USA300JE2 WT, $\Delta merA$ and $\Delta hypR$ strains (OD_{550} 0.2) were mixed with HOSCN (200 μ M) in LB in (c) and the complemented strains WT+ empty plasmid (WT-pRB), $merA^+$, $merAC_{43}S$, $hypR^+$ in LB containing 1% xylose and 10 μ g/mL chloramphenicol in (d), then incubated at 37°C for 2 h. Every 30 min, bacteria were removed by centrifugation and HOSCN in the supernatant was measured by TNB assay as described in Material and Methods, and expressed relative to the starting concentration measured at the 0-time point. Symbols represent means \pm SD of at least three independent replicates. A significant difference between HOSCN remaining at each time point after addition to bacterial strains compared with media only was determined by a two-way ANOVA with Dunnett's multiple comparisons test and is indicated by * $p < 0.05$.

2.5 | HOSCN oxidizes HypR to intersubunit disulfides both in vitro and in vivo

We have previously shown that the HypR repressor senses HOCl stress by C_{33} - C_{99} intersubunit disulfide formation, leading to its inactivation and derepression of *merA* transcription (Loi et al., 2018a). The strong derepression of *merA* transcription under HOSCN stress indicates that the HypR repressor also forms an intermolecular disulfide in response to HOSCN. Non-reducing SDS-PAGE analysis showed that exposure of reduced HypR to increasing amounts of HOSCN in vitro resulted in the formation of disulfide-linked dimers migrating at the size of \sim 30 kDa (Figure 5b). The two closely migrating disulfide-cross-linked bands represent oxidized HypR with one and two C_{33} - C_{99} disulfide linkages (Loi et al., 2018a). HypR disulfides were fully reducible by DTT (Figure 5b).

To verify that HypR forms intersubunit disulfides in *S. aureus* in response to HOSCN in vivo, a *S. aureus* COL strain expressing His-tagged HypR was exposed to 100 μ M HOSCN. Protein extracts

were alkylated with NEM and subjected to non-reducing and reducing anti-His₆ immunoblot analyses (Figure 5c). While the majority of the HypR protein was reduced under non-stress conditions, HypR was fully oxidized to intersubunit disulfides following exposure to HOSCN, which were reversible under reducing conditions (Figure 5c). The partial oxidation of HypR observed in untreated WT cells might be caused by oxidants generated during aerobic growth or incomplete alkylation of HypR, which is overexpressed in the WT strain from plasmid pRB473.

To investigate whether HOSCN oxidation of HypR inhibits its repressor activity, we investigated the effect of HOSCN on the DNA-binding activity of HypR to the *hypR* promoter probe using gel electrophoretic mobility shift assays (EMSA). Incubation of the *hypR* promoter probe with reduced HypR resulted in a band shift compared with the free probe, indicating that HypR was fully bound to the *hypR* promoter (Figure 5d). HOSCN treatment resulted in the inhibition of the DNA-binding activity of HypR to the *hypR* promoter probe. The repressor activity of HOSCN-treated HypR could be restored upon reduction with DTT.

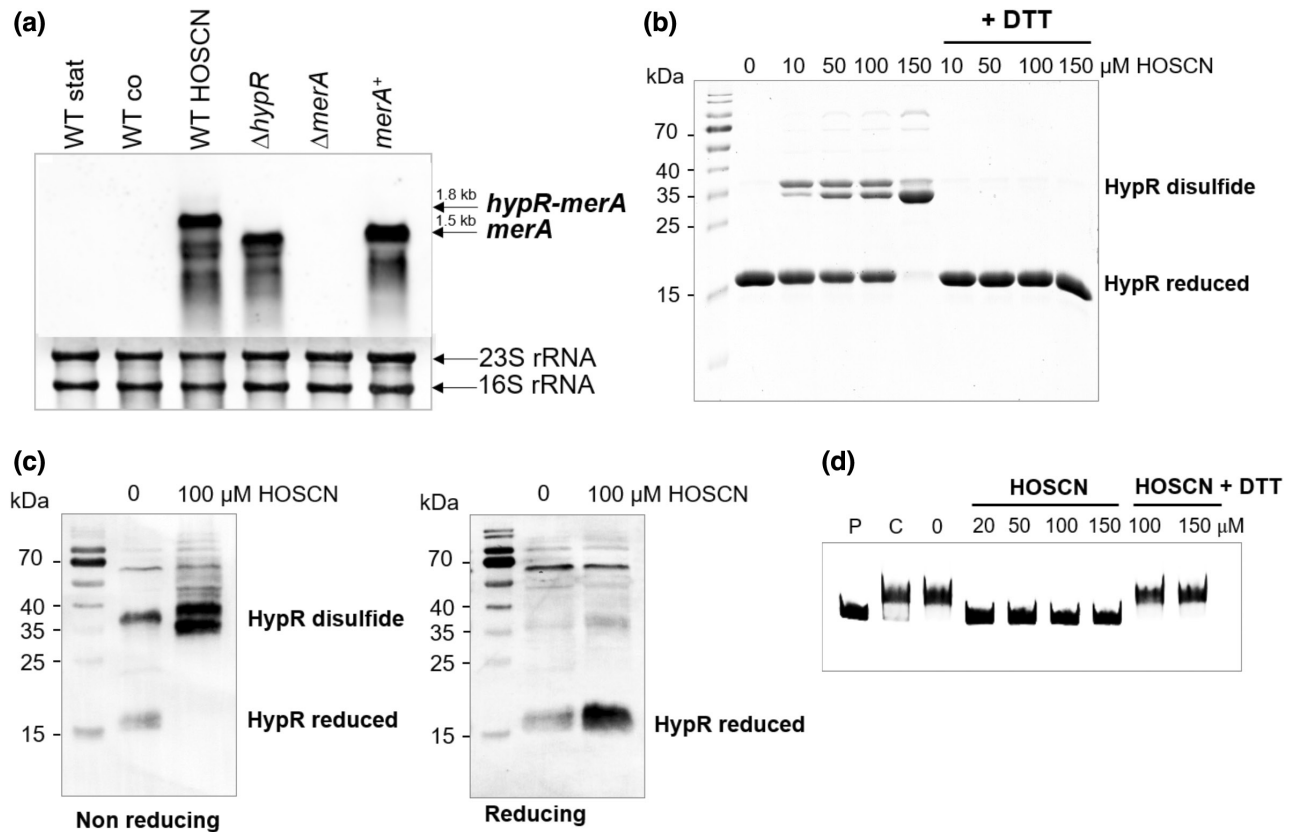


FIGURE 5 Transcription of *merA* is induced in *Staphylococcus aureus* upon HOSCN exposure through thiol-oxidation of the HypR repressor. (a) Northern blot analysis was performed using RNA isolated from *S. aureus* USA300JE2 strains after growth in LB medium using a *merA*-specific RNA probe as described previously (Loi et al., 2018a). Lanes 1–3 show transcription of the *hypR-merA* operon in stationary phase WT bacteria after 16 h growth and before and 30 min after exposure to 100 μ M HOSCN during exponential growth (OD_{550} of 0.4). Lanes 4–5 show transcription of *merA* in Δ *hypR* and Δ *merA* mutants at OD_{550} 0.4. Lane 6 shows transcription of *merA* in the *merA* complemented strain (*merA*⁺), grown in the presence of 1% xylose (OD_{550} of 0.4). The methylene blue stain shows the 16S and 23S rRNAs as RNA loading controls. (b) To study thiol-oxidation of HypR under HOSCN stress in vitro, purified His-tagged HypR protein (43 μ M) was pre-reduced with 10 mM DTT and oxidized by increasing doses of 10–150 μ M HOSCN for 15 min, followed by alkylation with 50 mM IAM for 30 min in the dark. HOSCN-oxidized HypR was also reduced with 20 mM DTT prior to alkylation with IAM. Samples were separated using non-reducing 15% SDS-PAGE and stained with Coomassie Blue. (c) To analyze thiol-oxidation of HypR in vivo, *S. aureus* COL expressing His-tagged HypR protein was harvested before and 30 min after treatment with 100 μ M HOSCN. NEM (50 mM) was added and protein extracts were subjected to non-reducing (left) and reducing (right) Western blot analysis using monoclonal anti-His₆ antibodies. The protein loading controls are shown as SDS-PAGE in Figure S3. (d) Electrophoretic mobility shift assays (EMSAs) were performed to analyze HypR-DNA-binding activity. Pre-reduced HypR protein (1 μ M) was exposed to increasing amounts of HOSCN (20–150 μ M) for 15 min prior to incubation with a *hypR* promoter DNA probe for 45 min. Oxidized HypR was also reduced with 10 mM DTT prior to incubation with the probe. The HypR-DNA-binding reactions were analyzed by EMSAs as described (Loi et al., 2018a). P indicates the free probe, C is the fully bound HypR-DNA complex. All images are representative of 3–4 independent replicates.

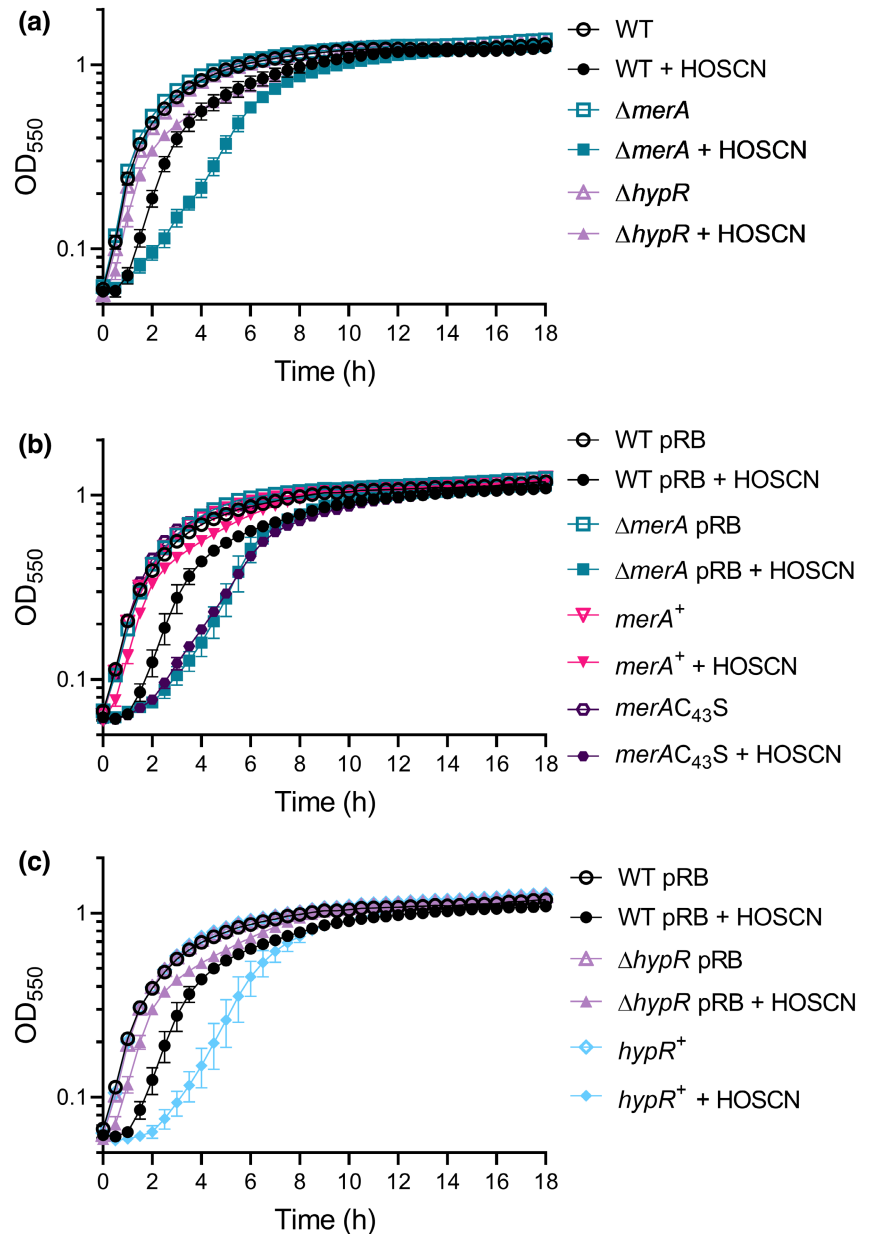
Collectively, these data demonstrate that HypR senses and responds to HOSCN stress by a thiol-switch mechanism to control *merA* expression in *S. aureus*.

2.6 | MerA confers tolerance of *S. aureus* to HOSCN

To determine whether MerA protects *S. aureus* against HOSCN, the growth phenotypes of JE2 mutant and complemented strains were assessed in the presence and absence of HOSCN. For this, we inoculated 96-well plates with exponential phase cultures

(Figure 6, Figure S4). While the addition of 50 μ M HOSCN did not affect bacterial growth (Figure S4), treatment with 100 and 200 μ M HOSCN resulted in a significantly reduced growth rate of the Δ *merA* mutant compared with WT (Figure 6a, Figure S4). The HOSCN tolerance of the *merA*⁺ complemented strain was equal to or greater than that of the WT strain at all HOSCN doses (Figure 6b, Figure S4). The Δ *merA* mutant complemented with the empty plasmid remained HOSCN-sensitive indicating that the plasmid alone and the presence of xylose and chloramphenicol in the growth assay does not affect HOSCN tolerance of *S. aureus* (Figure 6b). Similarly, growth of the Δ *merA* mutant was not restored by expression of the *merAC*_{43S} allele (Figure 6b, Figure S4),

FIGURE 6 MerA expression protects *Staphylococcus aureus* from HOSCN stress. Exponentially growing *S. aureus* USA300JE2 strains (OD_{550} 0.2) were grown in 96-well plates in the presence or absence of $100\mu\text{M}$ HOSCN in (a) LB or (b), (c) LB with 1% xylose and $10\mu\text{g/mL}$ chloramphenicol. OD_{550} measurements were taken every 30 min. Data are presented as mean \pm SD from at least three independent experiments, the y-axis is \log_{10} scale.



supporting that Cys_{43} is catalytically active. In addition, due to constitutive derepression of *merA*, the HOSCN tolerance of the $\Delta hypR$ mutant was equal to or greater than that of the WT strain at all HOSCN doses (Figure 6a, Figure S4). When complemented with empty plasmid, the same effect was observed (Figure 6c, Figure S4). Over-expression of HypR in the $hypR^+$ complemented strain led to a significant reduction in HOSCN tolerance compared with WT, and resulted in a growth phenotype similar to the $\Delta merA$ mutant (Figure 6c, Figure S4), highlighting the importance of this system for responding to HOSCN stress. To exclude low aeration in microplates as a confounding factor, we also assessed the growth of all strains in shaking flasks, which confirmed the observed growth phenotypes (Figure S5). Overall, our growth data support the role of the *hypR-merA* operon in protecting *S. aureus* from HOSCN.

3 | DISCUSSION

The present study shows that the flavoprotein disulfide reductase MerA functions as a HOSCN reductase in *S. aureus* and is important for defending against this innate immune-derived oxidant. Furthermore, we demonstrate that HOSCN oxidizes the redox-sensing regulator HypR to inhibit its repressor activity, resulting in the upregulation of *merA* transcription. In addition, high-resolution crystal structures of reduced $MerAC_{43}S$ and the oxidized MerA disulfide support the function of the enzyme as typical group-I FDR.

HOSCN is produced in human extracellular fluids through the oxidation of SCN^- by heme peroxidases. Our HOSCN killing data demonstrate that *S. aureus* can tolerate exposure of up to $800\mu\text{M}$ of HOSCN for >3 h. Concentrations of SCN^- can reach 600 – $800\mu\text{M}$ in the respiratory tract (Lorentzen et al., 2011; Wijkstrom-Frei

et al., 2003). However, due to limitations in H_2O_2 availability and the presence of competing HOSCN targets, the highest HOSCN concentration tested here represents the upper limit of what *S. aureus* will likely encounter in vivo. *S. aureus* survived 10–30-fold higher doses of HOSCN than *P. aeruginosa*, which does not colonize the respiratory tract of healthy people. Furthermore, *S. aureus* tolerated similar exposure times (>150 min) as previously reported for *S. pneumoniae* (Shearer et al., 2022c), another nasopharyngeal commensal and lung pathogen. In contrast, all of these bacteria succumb to comparable low doses and exposure times of HOCl (LD_{50} 3–10 nmol/ 10^8 bacteria, <60 min) (Shearer et al., 2021; Shearer et al., 2022a). Our findings suggest that targeting bacterial HOSCN defense mechanisms of respiratory pathogens holds promise for novel therapeutics.

A large body of work has focused on how *S. aureus* resists the oxidative burst of macrophages and neutrophils (Ashby et al., 2022; de Jong et al., 2019; Loi et al., 2018a). In this context, *merA* was noticed to be strongly upregulated in the transcriptome under neutrophil infections (Voyich et al., 2005). We have previously characterized HypR as a HOCl-sensitive repressor that controls *merA* transcription and identified the FDR as an important survival mechanism of *S. aureus* under HOCl stress and macrophage infections (Loi et al., 2018a). The *hypR-merA* operon is the only target for repression by HypR. *S. aureus* MerA has also been shown to play a role in detoxifying the thiol-reactive antimicrobial organosulfur compound allicin by acting as NADPH-dependent allicin reductase (Loi et al., 2019), and is important for the bacteria's defense against diamide and the oxidative stress-inducing metal-based antimicrobial AGXX® surface coating (Loi et al., 2018a; Loi et al., 2018b). We now report that the *hypR-merA* operon responds strongly to sub-lethal concentrations of immune-derived HOSCN, conferring tolerance of *S. aureus* to this thiol-specific oxidant. Collectively, these studies point to the essential role of MerA for *S. aureus* to tolerate immune-derived oxidants and thiol-active antimicrobials.

MerA was previously annotated as mercuric reductase based on some homology to group-II FDR enzymes that can reduce Hg^{2+} to Hg^0 , including P00392 of *Pseudomonas aeruginosa* (<30% sequence identity). However, in *P. aeruginosa* MerA, the Hg^{2+} is coordinated by two C-terminal Cys residues (Cys₅₅₈–Cys₅₅₉) (Argyrou & Blanchard, 2004), which are absent in the *S. aureus* MerA protein and in the closely related HOSCN reductases RclA of *E. coli* and Har of *S. pneumoniae* (Figure S1), making them unlikely to be efficient Hg^{2+} reductases. Indeed, studies with recombinant RclA reported that the NADH oxidation rate was 500-fold faster in the presence of HOSCN compared with Hg^{2+} (or Cu^{2+}) (Baek et al., 2020). In addition, mercury will be not encountered during the interaction of *S. aureus* with the host immune system, indicating that a function of MerA as mercuric reductase is not physiologically relevant.

The finding that MerA, RclA, and Har function as HOSCN reductases raises the question of whether they can also reduce HOCl, which would explain why these enzymes confer protection against this oxidant (Loi et al., 2018a; Parker et al., 2013). HOCl reductase activity is difficult to ascertain experimentally due to the high reactivity of HOCl with the enzyme and the pyridine nucleotide cofactor.

In addition, whether these FDRs are present at high enough concentrations in bacteria to compete against more abundant targets for HOCl is uncertain. Quantitative redox proteomics did not identify RclA as a significantly oxidized protein in *E. coli* following HOCl exposure (Leichert et al., 2008). Protection against HOCl may also be mediated by these FDRs through the reduction of secondary chloramines, which are formed when HOCl reacts with abundant protein amine groups, and like HOSCN, are more thiol-selective oxidants than HOCl (Pattison & Davies, 2006). Indeed, RclA showed some reductase activity with taurine and glycine chloramine, but this was orders of magnitude slower than with HOSCN (Meredith et al., 2022), suggesting specificity of these enzymes for HOSCN among reactive (pseudo-)halogen species. More comprehensive studies with recombinant MerA are needed to compare kinetic parameters with a variety of substrates to clarify whether this enzyme is a broad-spectrum or promiscuous defense system, or whether its reactivity with HOSCN clearly outstrips its performance against other thiol-reactive agents, such as allicin or diamide.

The MerA structures reported here are consistent with the catalytic mechanism of a typical group I FDR, whereby the C-terminal cysteine of the conserved CXXXXC motif interacts with $FADH_2$ in the reductive half-reaction, followed by electron transfer to the redox-active disulfide (Figure S6) (Argyrou & Blanchard, 2004). Moreover, the view into the active site of the MerAC₄₃S structure revealed that the C/S₄₃XXXXC₄₈ motif in one subunit is in close contact to the H₄₂₇XXXXE₄₃₂ motif of the opposing subunit (Figure 2c). The imidazole ring of H₄₂₇ interacts with the active site C₄₃S (2.8 Å), likely assisting the deprotonation of C₄₃ to the reactive thiolate anion by acting as a proton acceptor (Figure 2c, Figure S6). Both RclA and MerA have the conserved K₁₃ and K₁₆ residues at the entrance of the active site that are unique to this family of enzymes (Figure 2c, Figures S1 and S2), creating a positively charged environment that has been previously suggested to be important for substrate binding (Baek et al., 2020). Specificity for HOSCN may be conferred by these lysine residues through favoring binding of negatively charged substrates. Unlike chloramines and HOCl, HOSCN is predominantly present in its deprotonated form as OSCN[−] at physiological pH (>99%). Once in the active site, OSCN[−] can accept a proton from H₄₂₇ and react with the C₄₃ thiolate to form a sulfenyl thiocyanate intermediate, which is known to occur upon thiol-oxidation by HOSCN (Figure S6) (Aune & Thomas, 1978; Thomas & Aune, 1978). To complete the oxidative half-reaction, this intermediate will be resolved through a nucleophilic attack from the adjacent C₄₈ to generate the C₄₃–C₄₈ disulfide and to release SCN[−] (Figure S6), which is known to be generated during the catalytic cycle of RclA (Meredith et al., 2022).

As in our present study with MerA, deletion of RclA sensitizes *E. coli* to HOSCN stress (Meredith et al., 2022). Furthermore, heterologous expression of *S. aureus* MerA in the *E. coli* $\Delta rclA$ mutant reversed the increased HOSCN sensitivity caused by *rclA* deletion (Meredith et al., 2022), supporting our present finding that MerA acts as a protective mechanism against HOSCN. Even though our *S. aureus* growth experiments were conducted in rich LB medium, which is likely to have

more HOSCN-reactive thiols than the M9 minimal medium used in the *E. coli* study, the protective effect of MerA was detected at 6–8-fold lower HOSCN concentrations than those reported for RclA in *E. coli* (100–200 vs. 600–800 μ M) (Meredith et al., 2022). This observation might point to differences in expression levels of the two enzymes following HOSCN exposure, NAD(P)H availability, or the relative importance of the reductase enzyme compared with other antioxidant systems in the two bacteria. These differences might also reflect differences in HOSCN levels at their respective sites of colonization and other environmental habitats. *E. coli* colonizes and infects the human gut, where SCN^- levels are lower than in the respiratory tract (250–300 vs. 600–800 μ M, respectively) (Das et al., 1995). HOSCN will be generated at this site by MPO released from neutrophils in conditions such as inflammatory bowel disease (IBD) (Hansberry et al., 2017). Assuming gut concentrations of 100 mM chloride and 300 μ M SCN^- , about 70% of the available H_2O_2 will be used by MPO to generate HOSCN (van Dalen et al., 1997). Overall, the HOSCN concentrations in the gut are unlikely to reach as high a concentration as in the respiratory tract. In vivo studies examining the virulence and survival of the respective *rclA* and *merA* deletion mutants during infections are needed to establish the importance of these enzymes in protection against immune-derived oxidants generated at different sites. Furthermore, MerA/RclA enzymes are highly conserved in bacteria colonizing epithelial surfaces, including the phyla Actinobacteria, Bacteroidetes, Firmicutes, Fusobacteria, and Proteobacteria (Derke et al., 2020), but their role remains to be demonstrated.

Unlike MerA and RclA, which are highly inducible in *S. aureus* and *E. coli* in response to reactive (pseudo-)halogen species (present study, Loi et al., 2018a; Parker et al., 2013), via the redox-sensitive regulators HypR and RclR, respectively, transcription of *har* was not elevated in *S. pneumoniae* after HOCl stress (Fritsch et al., 2022). In support of this, *har* (*SPD_1415*) is not located adjacent to a putative regulatory gene in the *S. pneumoniae* genome, as indicated by the KEGG pathway database. Our comparative HOSCN survival data reflects the ability of *S. aureus*, but not *S. pneumoniae* to increase the expression of their respective HOSCN detoxifying enzyme: *S. pneumoniae* eventually die when exposed continuously to HOSCN in buffer (Figure 1a) (Shearer et al., 2022c), where the oxidant concentration is relatively stable (Shearer et al., 2022a). In contrast, the present investigation shows that around half of the *S. aureus* cells are still viable after 3 h in the same system likely owing to their ability to upregulate *merA* and to detoxify HOSCN. However, future studies are required to better understand transcriptional regulation of *har* in *S. pneumoniae*.

Comparing the kinetics of HOSCN disappearance from media in the presence and absence of *S. aureus* provides insight into the mechanistic action of the oxidant. After 30 min, the HOSCN concentration in media alone was 60%, dropping to 30% after 60 min, due to degradation or reaction with media constituents. In the presence of WT bacteria, the loss of HOSCN was not substantially faster. This finding is consistent with our observations in *S. pneumoniae* and *P. aeruginosa* (Shearer et al., 2022a) and can be ascribed to HOSCN (pK_a 4.8) being largely present as the membrane-impermeable OSCN^- (>99%) at physiological pH. While the small amount of uncharged HOSCN that

can permeate the cell was near the detection limit of our assay, it was enough to decrease the bacterial growth rate by approximately the amount of the time it took for HOSCN to be removed from the media. Growth of the $\Delta merA$ mutant was impaired by HOSCN more than in the WT, suggesting that in WT bacteria, MerA protects critical thiol targets from oxidation by decreasing the intracellular HOSCN concentration. Slowed growth in the presence of HOSCN was also observed in the $\Delta hypR^+$ mutant and when the $\Delta merA$ mutant was complemented with the empty plasmid or with the *merAC*_{43S} allele. Further, constitutive expression of MerA by *hypR* deletion or *merA*⁺ complementation improved growth relative to the WT strain in the presence of HOSCN by enabling the oxidant to be metabolized immediately upon exposure. In support of this, we detected a greater loss of HOSCN from the media in the *merA*⁺ complemented strain and in the $\Delta hypR$ mutant. The $\Delta merA$ mutant eventually reached stationary phase at the same OD as the other strains, consistent with the predominantly reversible protein thiol-oxidation that was previously measured in *E. coli* exposed to HOSCN (Thomas & Aune, 1978). Here we show that HOSCN is nearly completely consumed by the media after 2 h, after which reversibly oxidized thiols can be reduced in order for cells to resume growth. In contrast to our bolus HOSCN experiments, *S. aureus* will be exposed to a continuous flux of HOSCN in vivo, where greater growth inhibition or even bacterial killing due to irreversible thiol-oxidation might be achieved if MerA was rendered dysfunctional.

In addition to MerA, *S. aureus* is likely to have other HOSCN defenses. In *S. pneumoniae*, we have shown that HOSCN reductase activity alone is insufficient to protect against this oxidant and that additionally the glutathione/glutathione reductase system is required for protection, with the pneumococci being completely sensitized to HOSCN when both systems are deleted (Shearer et al., 2022b). As a glutathione surrogate, *S. aureus* uses bacillithiol (BSH) as a major low molecular weight thiol and antioxidant (Newton et al., 2009). BSH and the bacilliredoxin (Brx)/BSH/bacillithiol disulfide reductase (YpdA) redox system have been shown to protect *S. aureus* against HOCl and H_2O_2 stress and from leukocyte killing (Ashby et al., 2022; Linzner et al., 2019; Linzner et al., 2021; Posada et al., 2014). Whether BSH and the Brx/BSH/YpdA system also contribute to HOSCN tolerance warrants further investigation.

In conclusion, we show that MerA functions as a HOSCN reductase in *S. aureus* and contributes to its high tolerance of HOSCN. Targeting HOSCN defenses in *S. aureus* might be a novel strategy for treating this multi-drug resistant pathogen. While the present study identifies MerA as a potential target in this context, future studies should endeavor to identify any additional HOSCN resistance mechanisms in *S. aureus*.

4 | EXPERIMENTAL PROCEDURES

4.1 | Materials

Lysostaphin (from *Staphylococcus staphylolyticus*), LPO from bovine milk ($\epsilon 412 = 112,000/\text{M}/\text{cm}$ (Paul & Ohlsson, 1985)), ethylenediamine tetraacetic acid (EDTA), chloramphenicol, D-(+)-xylose

isopropyl- β -D-thiogalactopyranoside (IPTG), dithiothreitol (DTT), N-ethylmaleimide (NEM), iodoacetamide (IAM), anti-mouse IgG (Fab-specific)-alkaline phosphatase conjugated secondary antibodies (Cat. No. A1293) and Amicon Ultra 0.5 centrifugal filter units (MWCO 10 kDa) were purchased from Sigma-Aldrich (Merck). Hank's balanced salt solution (HBSS) and phosphate-buffered saline (PBS) for cell culture, both Gibco, and the anti-His₆ monoclonal antibodies (4E3D10H2/E3, Invitrogen) were purchased from Thermo Fisher. Hydrogen peroxide (30%) (H₂O₂, $\epsilon_{240} = 43.6/\text{M}/\text{cm}$ (Beers & Sizer, 1952)) was from LabServ. 2-Nitro-5-thiobenzoate (TNB) was prepared from 5,5'-dithiobis-(2-nitrobenzoic acid) (DTNB, Sigma-Aldrich) through alkaline hydrolysis as described (Nagy et al., 2009). HOSCN was generated and quantified as described in (Shearer et al., 2022a), kept on ice and used within 30 min of quantification. Nicotinamide adenine dinucleotide phosphate (NADPH) was purchased from Carbosynth.

4.2 | Bacterial strains

The bacterial strains used for this study were *S. pneumoniae* strain D39 serotype 2 (NCTC 7466), *P. aeruginosa* PAO1 (ATCC 47085), *S. aureus* USA300 (Tenover et al., 2006), USA300JE2 (Fey et al., 2013), and COL (Shafer & Landolo, 1979) wild-type strains. In addition, we constructed USA300JE2 $\Delta merA$ and $\Delta hypR$ mutants, WT-pRB473, *merA*⁺, $\Delta merA$ -*merAC*_{43S}, $\Delta merA$ -pRB473, *hypR*⁺ and $\Delta hypR$ -pRB473 complemented strains (Table S2). Mutant strains were generated as described for the *S. aureus* COL background (Loi et al., 2018a). The *S. aureus* USA300JE2 $\Delta merA$ and $\Delta hypR$ strains were constructed using the previously generated plasmids pMAD-delta-*merA* and pMAD-delta-*hypR*, respectively. USA300JE2 complemented strains carry the ectopic plasmid pRB473 with or without a gene of interest that is expressed under the control of a xylose-inducible promoter using chloramphenicol resistance for selection (Loi et al., 2018a). For Western Blot analyses, the COL-pRB473-*hypR*-*His* complemented strain was used (Linzer et al., 2020).

All WT bacterial strains were stored under standard conditions, maintained on Columbia or tryptic soy broth sheep blood agar plates (Fort Richard Laboratories) and with the exception of *S. pneumoniae*, were cultivated in Luria Broth medium (LB, Miller's, Thermo Fisher Scientific) at 37°C under vigorous agitation at 200 rpm. *S. pneumoniae* was statically grown overnight at 37°C with 5% CO₂ in brain heart infusion media (Oxoid, Thermo Fisher Scientific), then diluted in fresh media and grown to an OD₆₂₀ of 0.4–0.7 before the experiments. Complemented strains containing the pRB473 plasmid were cultivated on LB plates or in LB media containing 1% xylose and 10 $\mu\text{g}/\text{mL}$ chloramphenicol.

4.3 | HOSCN killing assays

Bacterial cultures were centrifuged at 12,000 g for 5 min, and bacterial pellets were washed twice with PBS, then suspended in HBSS,

pH 6.8. In the case of *S. aureus* and *P. aeruginosa*, biofilms and bacterial aggregates were removed by a slow spin at 100g for 5 min. The OD was measured and the concentration of bacteria (colony forming units (CFU)/mL) was determined from a standard curve. Bacteria were incubated at a concentration of 2.5×10^5 CFU/mL with 0–800 μM HOSCN in HBSS, pH 6.8 for up to 3 h at 37°C with 5% CO₂. This pH was chosen to more closely resemble that of respiratory tract fluids (Fischer & Widdicombe, 2006; Zajac et al., 2021). For time course experiments, samples were taken at 30 min intervals, serially diluted in PBS for *P. aeruginosa* and *S. pneumoniae*, and in pH 11, water for *S. aureus*, and plated on blood agar plates.

4.4 | HOSCN reductase activity in bacterial lysates

Bacteria were pelleted by centrifugation at 10,000 g for 50 min at 4°C, washed once with PBS, then resuspended in 1–5 mL of 100 mM phosphate buffer (pH 7.4) containing 1 mM EDTA. *P. aeruginosa* was lysed by pulse sonication on ice for 5 min. *S. aureus* was lysed by adding lysostaphin at 10–30 $\mu\text{g}/\text{mL}$ to resuspended pellets and incubating for 15–20 min at 37°C. Bacterial debris was removed by centrifugation at 10,000 g for 10 min at 4°C. The consumption of NADPH (200 μM) by bacterial lysates (200 μL) after the addition of HOSCN (100 μM) or buffer was measured in 100 mM phosphate buffer (pH 7.4) containing 1 mM EDTA (reductase buffer) by monitoring the loss of absorbance at 340 nm using an UV-visible spectrophotometer. For the USA300JE2 *merA*⁺ complemented strain and the $\Delta hypR$ mutant, diluted lysates (1:80 or 1:40, respectively) were used in the assay. The protein concentration in bacterial lysates was determined by Bradford assay (Bradford, 1976). Reductase activity was defined as the rate of NADPH consumption and was calculated using $\epsilon_{340} = 6220/\text{M}/\text{cm}$ for NADPH (Horecker & Kornberg, 1948) and the following formula

$$\begin{aligned} \text{Reductase activity } (\mu\text{mol}/\text{min}/\text{mg}) \\ = \Delta\text{Abs}_{340} / (\Delta t \times 6220 / (\text{M} \times \text{cm})) \times 1 \text{ cm} \times c_{\text{protein}} \end{aligned}$$

4.5 | Expression and purification of His-tagged MerA, MerAC_{43S}, and HypR proteins

Construction of *E. coli* BL21DE3 *plysS* strains (Merck Millipore) expressing plasmids pET11b-*hypR*, pET11b-*merA*, and pET11b-*merAC*_{43S} and purification of recombinant His-tagged HypR, MerA, and MerAC_{43S} proteins were described previously (Loi et al., 2018a). Cultivation was performed in 1.5 L LB medium until an OD₆₀₀ of 0.8, followed by the addition of 1 mM IPTG and incubation for 3.5 h at 37°C to induce HypR expression and for 16 h at 25°C to induce MerA and MerAC_{43S} expression. His-tagged HypR, MerA, and MerAC_{43S} proteins were purified using His Trap™ HP Ni-NTA columns (Thermo Fisher Scientific) with the ÄKTA purifier liquid chromatography system (Amersham Biosciences Europe GmbH) as previously described (Loi et al., 2018a).

For crystallization, MerA and MerAC_{43S} were subjected to size-exclusion chromatography using a HiLoad 26/600 Superdex 200

column (Cytiva) connected to an Äkta PURE chromatography system (Cytiva). The column was equilibrated with 20 mM HEPES pH 7.5, 20 mM KCl and 200 mM NaCl. Peak fractions were concentrated to a final concentration of 1 mM using Amicon Ultra-30K centrifugal filters (Merck Millipore) and subjected to crystallization experiments.

4.6 | Protein crystallization

Crystallization was performed using the sitting-drop method at 20°C in 0.5–0.75 μ L drops. The drops consisted of either 1:1 or 1:2 ratios of protein and precipitant solutions. Crystallization drops were set automatically using the Crystal Gryphon robot (Art Robbins Instruments). NeXtal JCSG suites I–IV and Classics II were used to screen for crystallization conditions. MerA crystallized at 1 mM concentration within 7 days in 0.1 M citrate pH 4.0, 5% (w/v) PEG 6000; pH 5.0. MerAC₄₃S crystallized at 1 mM concentration within 7 days in 0.2 M diammonium tartrate, 20% (w/v) PEG 3350. The crystallographic data collection and refinement statistics are given in Table S1.

4.7 | Structure analysis of MerA and MerAC₄₃S proteins by X-ray crystallography

Prior to data collection, the crystals were flash-frozen in liquid nitrogen employing a cryosolution that consisted of crystallization solution supplemented with 15% (v/v) glycerol. The data were collected under cryogenic conditions at the EMBL beamline P13 (Deutsches Elektronen Synchrotron; DESY). The data were integrated and scaled using XDS and merged with XSCALE (Kabsch, 2010). The structure of MerA was determined by molecular replacement (MR) in PHASER (McCoy et al., 2007) using 1EBD as the search model. The structure of MerAC₄₃S was determined by MR using the structure of MerA as the search model. Both structures were manually built in COOT (Emsley & Cowtan, 2004), and refined with PHENIX (Adams et al., 2010). The figures were prepared with PyMOL (Delano, 2002). The structure factors and atomic coordinates have been deposited in the RSCB Protein Data Bank (<https://www.rcsb.org>) under accession numbers 8AJJ for MerA and 8AJK for MerAC₄₃S.

4.8 | Transcriptional analysis of the *hypR-merA* operon using northern blot analyses

Staphylococcus aureus USA300JE2 WT, Δ *hypR* and Δ *merA* mutants as well as the *merA*⁺ complemented strains were grown in LB under vigorous agitation at 37°C to exponential phase at an optical density at 550 nm (OD₅₅₀) of 0.4. The WT strain was harvested before and 30 min after exposure to 100 μ M HOSCN at an OD₅₅₀ of 0.4. The untreated *S. aureus* mutants and complemented strains were harvested at an OD₅₅₀ of 0.4. The cells were disrupted in 3 mM EDTA, 200 mM NaCl lysis buffer with a Precellys24 Ribolyzer (Bertin Instruments)

and RNA isolation was performed using the acid phenol extraction method as previously described (Loi et al., 2018a; Wetzstein et al., 1992). Northern blot hybridization was performed using the *merA*-specific digoxigenin-labeled antisense RNA probe generated by in vitro transcription as described (Loi et al., 2018a; Wetzstein et al., 1992).

4.9 | Electrophoretic mobility shift assays (EMSA) to investigate the effect of HOSCN on the DNA-binding activity of HypR to the *hypR* promoter probe

Pre-reduced HypR protein (1 μ M) was treated with increasing amounts of HOSCN (20–150 μ M) for 15 min, followed by incubation with or without 10 mM DTT, prior to incubation with the *hypR* promoter probe for 45 min as described previously (Loi et al., 2018a). The *hypR* promoter probe covered the *hypR* upstream region of –128 to +70 relative to the transcriptional start site containing the inverted repeat sequence as HypR operator as described Loi et al. (2018a). The HypR-DNA-binding reactions were analyzed by 4% native polyacrylamide gel electrophoresis and stained using SYBR green (Thermo Fisher Scientific) as described Loi et al. (2018a).

4.10 | Non-reducing SDS-PAGE to analyze HypR oxidation by HOSCN in vitro

Purified HypR protein was pre-reduced with 10 mM DTT for 20 min at RT, followed by DTT removal with Micro Biospin 6 columns (Biorad). Reduced HypR (43 μ M) was oxidized with 10, 50, 100, and 150 μ M HOSCN for 15 min, followed by alkylation with 50 mM IAM for 30 min in the dark. To determine reversible thiol-oxidation of HypR, 20 mM DTT was added and incubated for 15 min prior to IAM alkylation. Reduced and oxidized HypR proteins were separated by 15% non-reducing and reducing SDS-PAGE and stained with Coomassie Blue as described previously Loi et al. (2018a).

4.11 | His-tag-specific Western blot analysis to analyze HypR oxidation by HOSCN in vivo

Staphylococcus aureus COL WT expressing His-tagged HypR on plasmid pRB473-*hypR*-His (Linzner et al., 2020) was grown in LB to an OD₅₅₀ of 2. Cells were harvested by centrifugation, washed with Belitsky minimal medium (BMM) (Stulke et al., 1993) and adapted to BMM for 1 h before exposure to 100 μ M HOSCN for 30 min as described previously Loi et al. (2018a). Cells were washed in Tris-EDTA-buffer (10 mM Tris, 1 mM EDTA, pH 8.0) with 50 mM NEM, disrupted using the ribolyzer and the protein extract was cleared from cell debris by repeated centrifugation. Protein amounts of 25 μ g were diluted in non-reducing or reducing SDS sample buffer, separated using 15% SDS-PAGE followed by Western blot analysis using anti-His₆ monoclonal antibodies and anti-mouse IgG

(Fab-specific)-alkaline phosphatase conjugated secondary antibodies as described previously (Chi et al., 2013; Van Loi et al., 2021). To confirm equal protein loading, protein extracts were also analyzed by SDS-PAGE and stained with Coomassie.

4.12 | HOSCN consumption by bacteria growing in LB

USA300JE2 WT and mutant strains were grown in LB overnight, diluted to an OD₅₅₀ of 0.1, and then grown to an OD₅₅₀ of 1. Complemented strains were grown in LB supplemented with 1% xylose and 10 µg/mL chloramphenicol to the same OD. Bacteria were centrifuged at 100 g for 5 min to remove biofilm and bacterial aggregates, before measuring bacterial density at OD₅₅₀. Bacteria (OD₅₅₀ 0.2) were incubated with HOSCN (200 µM) at 37°C for 2 h in LB or LB with 1% xylose and 10 µg/mL chloramphenicol for complemented strains. Every 30 min, a 100 µL sample was removed and bacteria were pelleted by centrifugation (5 min, 12,000 g). The HOSCN remaining in the supernatant was measured by TNB assay. A volume of 30 µL of the reaction mixture was added to 970 µL of 50–60 µM TNB. The absorbance change at 412 nm was used to measure the HOSCN concentration present in the mixture using $\epsilon_{412} = 14,100/\text{M}/\text{cm}$ for TNB and accounting for the fact that 1 mole HOSCN causes the loss of 2 moles of TNB. A media only sample was used as a control and subtracted from all other values.

4.13 | Bacterial growth in the presence of HOSCN

Exponentially growing USA300JE2 strains were prepared as described in the HOSCN consumption assay. Bacteria (OD₅₅₀ 0.2) were exposed to 0, 50, 100, and 200 µM HOSCN in a 96-well plate alongside media only controls (150 µL/well). Growth was measured every 30 min at 37°C with shaking for 18 h in a BioTek Synergy Neo2 Hybrid Multi-Mode Microplate Reader. Values for media only were subtracted from all measurements.

4.14 | Statistical analyses

Graphs were plotted and the statistical analyses stated in the figure legends were performed using GraphPad Prism (Version 8.2.1). A $p < 0.05$ was considered significant.

AUTHOR CONTRIBUTIONS

N.D., H. A.: conceptualization. H.L.S., L.V.V., N.D.: investigation. H.L.S., L.V.V., N.D., H.A.: formal analysis. P.W., G.B., F.A.: X-ray crystallography. H.L.S., N.D.: writing – first draft. N.D., H.A., M.B.H.: funding acquisition. H.A., M.B.H.: writing – review & editing.

ACKNOWLEDGMENTS

We are grateful to Professor Tony Kettle and Dr Michael Currie for their scholarly input. This study was supported by the Canterbury

Medical Research Foundation (Project Grant #05/20), a University of Otago Research Grant (#3579) and a Sir Charles Hercus Health Research Fellowship from the Health Research Council of New Zealand to N. D. This work was further supported by grants from the Deutsche Forschungsgemeinschaft (AN746/4-1 and AN746/4-2) within the SPP1710 on “Thiol-based Redox switches,” by the SFB973 project C08 and TR84 project B06 to H.A. P.W. acknowledges funding from the Deutsche Forschungsgemeinschaft within the GRK 2573. Open access publishing facilitated by University of Otago, as part of the Wiley - University of Otago agreement via the Council of Australian University Librarians.

CONFLICT OF INTEREST STATEMENT

The authors have no conflict of interest to declare.

DATA AVAILABILITY STATEMENT

The data that support the findings of this study are available from the corresponding author upon reasonable request.

ORCID

Heather L. Shearer  <https://orcid.org/0000-0001-8191-7723>

Gert Bange  <https://orcid.org/0000-0002-7826-0932>

Mark B. Hampton  <https://orcid.org/0000-0002-7349-3729>

Haike Antelmann  <https://orcid.org/0000-0002-1766-4386>

Nina Dickerhof  <https://orcid.org/0000-0003-2269-4595>

REFERENCES

- Adams, P.D., Afonine, P.V., Bunkóczi, G., Chen, V.B., Davis, I.W., Echols, N. et al. (2010) PHENIX: a comprehensive python-based system for macromolecular structure solution. *Acta Crystallographica Section D: Biological Crystallography*, 66(Pt 2), 213–221.
- Argyrou, A. & Blanchard, J.S. (2004) Flavoprotein disulfide reductases: advances in chemistry and function. *Progress in Nucleic Acid Research and Molecular Biology*, 78, 89–142.
- Ashby, L.V., Springer, R., van Loi, V., Antelmann, H., Hampton, M.B., Kettle, A.J. et al. (2022) Oxidation of bacillithiol during killing of *Staphylococcus aureus* USA300 inside neutrophil phagosomes. *Journal of Leukocyte Biology*, 112, 591–605.
- Aune, T.M. & Thomas, E.L. (1978) Oxidation of protein sulfhydryls by products of peroxidase-catalyzed oxidation of thiocyanate ion. *Biochemistry*, 17(6), 1005–1010.
- Baek, Y., Kim, J., Ahn, J., Jo, I., Hong, S., Ryu, S. et al. (2020) Structure and function of the hypochlorous acid-induced flavoprotein RclA from *Escherichia coli*. *The Journal of Biological Chemistry*, 295(10), 3202–3212.
- Beers, R.F. & Sizer, I.W. (1952) A spectrophotometric method for measuring the breakdown of hydrogen peroxide by catalase. *Journal of Biological Chemistry*, 195(1), 133–140.
- Bradford, M.M. (1976) A rapid and sensitive method for the quantitation of microgram quantities of protein utilizing the principle of protein-dye binding. *Analytical Biochemistry*, 72, 248–254.
- Carlsson, J., Iwami, Y. & Yamada, T. (1983) Hydrogen peroxide excretion by oral streptococci and effect of lactoperoxidase-thiocyanate-hydrogen peroxide. *Infection and Immunity*, 40(1), 70–80.
- Chi, B.K., Roberts, A.A., Huyen, T.T.T., Bäsell, K., Becher, D., Albrecht, D. et al. (2013) S-bacillithiolation protects conserved and essential proteins against hypochlorite stress in firmicutes bacteria. *Antioxidants & Redox Signaling*, 18(11), 1273–1295.

- van Dalen, C.J. & Kettle, A.J. (2001) Substrates and products of eosinophil peroxidase. *The Biochemical Journal*, 358(Pt 1), 233–239.
- van Dalen, C.J., Whitehouse, M.W., Winterbourn, C.C. & Kettle, A.J. (1997) Thiocyanate and chloride as competing substrates for myeloperoxidase. *The Biochemical Journal*, 327(Pt 2), 487–492.
- Das, D., De, P.K. & Banerjee, R.K. (1995) Thiocyanate, a plausible physiological electron donor of gastric peroxidase. *The Biochemical Journal*, 305(Pt 1), 59–64.
- Day, B.J., Bratcher, P.E., Chandler, J.D., Kilgore, M.B., Min, E., LiPuma, J.J. et al. (2020) The thiocyanate analog selenocyanate is a more potent antimicrobial pro-drug that also is selectively detoxified by the host. *Free Radical Biology and Medicine*, 146, 324–332. Available from: <https://doi.org/10.1016/j.freeradbiomed.2019.11.016>
- Delano, W.L. (2002) *The PyMOL molecular graphics system*. DeLano Scientific. Available from <http://www.pymol.org>
- Derke, R.M., Barron, A.J., Billiot, C.E., Chaple, I.F., Lapi, S.E., Broderick, N.A. et al. (2020) The Cu(II) reductase RclA protects *Escherichia coli* against the combination of hypochlorous acid and intracellular copper. *MBio*, 11(5), e01905–e01920.
- Emsley, P. & Cowtan, K. (2004) Coot: model-building tools for molecular graphics. *Acta Crystallographica Section D: Biological Crystallography*, 60, 2126–2132.
- Fey, P.D., Endres, J.L., Yajjala, V.K., Widhelm, T.J., Boissy, R.J., Bose, J.L. et al. (2013) A genetic resource for rapid and comprehensive phenotype screening of nonessential *Staphylococcus aureus* genes. *mBio*, 4(1), e00537-12.
- Fischer, H. & Widdicombe, J.H. (2006) Mechanisms of acid and base secretion by the airway epithelium. *The Journal of Membrane Biology*, 211(3), 139–150.
- Fritsch, V.N., Linzner, N., Busche, T., Said, N., Weise, C., Kalinowski, J. et al. (2022) The MerR-family regulator NmlR is involved in the defense against oxidative stress in *Streptococcus pneumoniae*. *Molecular Microbiology*, 119, 191–207. Available from: <https://doi.org/10.1111/mmi.14999>
- Hampton, M.B., Kettle, A.J. & Winterbourn, C.C. (1998) Inside the neutrophil phagosome: oxidants, myeloperoxidase, and bacterial killing. *Blood*, 92(9), 3007–3017.
- Hansberry, D.R., Shah, K., Agarwal, P. & Agarwal, N. (2017) Fecal myeloperoxidase as a biomarker for inflammatory bowel disease. *Cureus*, 9(1), e1004.
- Harrison, J.E. & Schultz, J. (1976) Studies on the chlorinating activity of myeloperoxidase. *The Journal of Biological Chemistry*, 251(5), 1371–1374.
- Horecker, B.L. & Kornberg, A. (1948) The extinction coefficients of the reduced band of pyridine nucleotides. *The Journal of Biological Chemistry*, 175(1), 385–390.
- Horsburgh, M.J., Clements, M.O., Crossley, H., Ingham, E. & Foster, S.J. (2001) PerR controls oxidative stress resistance and iron storage proteins and is required for virulence in *Staphylococcus aureus*. *Infection and Immunity*, 69(6), 3744–3754.
- de Jong, N.W.M., Ramyar, K.X., Guerra, F.E., Nijland, R., Fevre, C., Voyich, J.M. et al. (2017) Immune evasion by a staphylococcal inhibitor of myeloperoxidase. *Proceedings of the National Academy of Sciences of the United States of America*, 114(35), 9439–9444.
- de Jong, N.W.M., van Kessel, K.P.M. & van Strijp, J.A.G. (2019) Immune evasion by *Staphylococcus aureus*. *Microbiology Spectrum*, 7(2). Available from: <https://doi.org/10.1128/microbiolspec.GPP3-0061-2019>
- Kabsch, W. (2010) XDS. *Acta Crystallographica Section D: Biological Crystallography*, 66(Pt 2), 125–132.
- Laux, C., Peschel, A. & Krismer, B. (2019) *Staphylococcus aureus* colonization of the human nose and interaction with other microbiome members. *Microbiology Spectrum*, 7(2). Available from: <https://doi.org/10.1128/microbiolspec.GPP3-0029-2018>
- Leichert, L.I., Gehrke, F., Gudiseva, H.V., Blackwell, T., Ilbert, M., Walker, A.K. et al. (2008) Quantifying changes in the thiol redox proteome upon oxidative stress in vivo. *Proceedings of the National Academy of Sciences of the United States of America*, 105(24), 8197–8202.
- Linzner, N., Loi, V.V., Fritsch, V.N., Tung, Q.N., Stenzel, S., Wirtz, M. et al. (2019) *Staphylococcus aureus* uses the bacilliredoxin (BrxAB)/bacillithiol disulfide reductase (YpdA) redox pathway to defend against oxidative stress under infections. *Frontiers in Microbiology*, 10, 1355.
- Linzner, N., Fritsch, V.N., Busche, T., Tung, Q.N., Loi, V.V., Bernhardt, J. et al. (2020) The plant-derived naphthoquinone lapachol causes an oxidative stress response in *Staphylococcus aureus*. *Free Radical Biology & Medicine*, 158, 126–136.
- Linzner, N., Loi, V.V., Fritsch, V.N. & Antelmann, H. (2021) Thiol-based redox switches in the major pathogen *Staphylococcus aureus*. *Biological Chemistry*, 402(3), 333–361.
- Loi, V.V., Busche, T., Tedin, K., Bernhardt, J., Wollenhaupt, J., Huyen, N.T.T. et al. (2018a) Redox-sensing under hypochlorite stress and infection conditions by the Rrf2-family repressor HypR in *Staphylococcus aureus*. *Antioxidants & Redox Signaling*, 29(7), 615–636.
- Loi, V.V., Busche, T., Preuß, T., Kalinowski, J., Bernhardt, J. & Antelmann, H. (2018b) The AGXX(R) antimicrobial coating causes a thiol-specific oxidative stress response and protein S-bacillithiolation in *Staphylococcus aureus*. *Frontiers in Microbiology*, 9, 3037.
- Loi, V.V., Huyen, N.T.T., Busche, T., Tung, Q.N., Gruhlke, M.C.H., Kalinowski, J. et al. (2019) *Staphylococcus aureus* responds to allicin by global S-thioallylation – role of the Brx/BSH/YpdA pathway and the disulfide reductase MerA to overcome allicin stress. *Free Radical Biology & Medicine*, 139, 55–69.
- Lorentzen, D., Durairaj, L., Pezzulo, A.A., Nakano, Y., Launspach, J., Stoltz, D.A. et al. (2011) Concentration of the antibacterial precursor thiocyanate in cystic fibrosis airway secretions. *Free Radical Biology and Medicine*, 50(9), 1144–1150.
- Mandell, G.L. (1975) Catalase, superoxide dismutase, and virulence of *Staphylococcus aureus*. In vitro and in vivo studies with emphasis on staphylococcal-leukocyte interaction. *The Journal of Clinical Investigation*, 55(3), 561–566.
- McCoy, A.J., Grosse-Kunstleve, R.W., Adams, P.D., Winn, M.D., Storoni, L.C. & Read, R.J. (2007) Phaser crystallographic software. *J Appl Crystallogr*, 40(Pt 4), 658–674.
- Meredith, J.D., Chapman, I., Ulrich, K., Sebastian, C., Stull, F. & Gray, M.J. (2022) *Escherichia coli* RclA is a highly active hypothiocyanite reductase. *Proceedings of the National Academy of Sciences of the United States of America*, 119(30), e2119368119.
- Nagy, P., Jameson, G.N. & Winterbourn, C.C. (2009) Kinetics and mechanisms of the reaction of hypothiocyanous acid with 5-thio-2-nitrobenzoic acid and reduced glutathione. *Chemical Research in Toxicology*, 22(11), 1833–1840.
- Newton, G.L., Rawat, M., la Clair, J.J., Jothivasan, V.K., Budiarto, T., Hamilton, C.J. et al. (2009) Bacillithiol is an antioxidant thiol produced in Bacilli. *Nature Chemical Biology*, 5(9), 625–627.
- Oram, J. & Reiter, B. (1966) The inhibition of streptococci by lactoperoxidase, thiocyanate and hydrogen peroxide. The effect of the inhibitory system on susceptible and resistant strains of group N streptococci. *Biochemical Journal*, 100(2), 373–381.
- Parker, B.W., Schwessinger, E.A., Jakob, U. & Gray, M.J. (2013) The RclR protein is a reactive chlorine-specific transcription factor in *Escherichia coli*. *The Journal of Biological Chemistry*, 288(45), 32574–32584.
- Pattison, D.I. & Davies, M.J. (2006) Reactions of myeloperoxidase-derived oxidants with biological substrates: gaining chemical insight into human inflammatory diseases. *Current Medicinal Chemistry*, 13(27), 3271–3290.
- Paul, K.G. & Ohlsson, P.I. (1985) In: Pruitt, K.M. & Tenovuo, J.O. (Eds.) *The lactoperoxidase system, chemistry and biological significance*. New York: Marcel Dekker, pp. 15–29.
- Pietrocola, G., Nobile, G., Rindi, S. & Speziale, P. (2017) *Staphylococcus aureus* manipulates innate immunity through own and host-expressed proteases. *Frontiers in Cellular and Infection Microbiology*, 7, 166.

- Posada, A.C., Kolar, S.L., Dusi, R.G., Francois, P., Roberts, A.A., Hamilton, C.J. et al. (2014) Importance of bacillithiol in the oxidative stress response of *Staphylococcus aureus*. *Infection and Immunity*, 82(1), 316–332.
- Sakr, A., Brégeon, F., Mège, J.L., Rolain, J.M. & Blin, O. (2018) *Staphylococcus aureus* nasal colonization: an update on mechanisms, epidemiology, risk factors, and subsequent infections. *Frontiers in Microbiology*, 9, 2419.
- Shafer, W.M. & landolo, J.J. (1979) Genetics of staphylococcal enterotoxin B in methicillin-resistant isolates of *Staphylococcus aureus*. *Infection and Immunity*, 25(3), 902–911.
- Shearer, H.L., Hampton, M.B. & Dickerhof, N. (2021) Bactericidal activity of the oxidants derived from mammalian heme peroxidases. In: Hawkins, C. & Nauseef, W.M. (Eds.) *Mammalian heme peroxidases, diverse roles in health and disease*. Boca Raton: CRC Press. Available from: <https://doi.org/10.1201/9781003212287>
- Shearer, H.L., Kaldor, C.D., Hua, H., Kettle, A.J., Parker, H.A. & Hampton, M.B. (2022a) Resistance of *Streptococcus pneumoniae* to hypothiocyanous acid generated by host peroxidases. *Infection and Immunity*, 90, e0053021.
- Shearer, H.L., Pace, P.E., Paton, J.C., Hampton, M.B. & Dickerhof, N. (2022b) A newly identified flavoprotein disulfide reductase Har protects *Streptococcus pneumoniae* against hypothiocyanous acid. *The Journal of Biological Chemistry*, 298, 102359.
- Shearer, H.L., Paton, J.C., Hampton, M.B. & Dickerhof, N. (2022c) Glutathione utilization protects *Streptococcus pneumoniae* against lactoperoxidase-derived hypothiocyanous acid. *Free Radical Biology & Medicine*, 179, 24–33.
- Shin, K., Hayasawa, H. & Lönnerdal, B. (2001) Inhibition of *Escherichia coli* respiratory enzymes by the lactoperoxidase-hydrogen peroxide-thiocyanate antimicrobial system. *Journal of Applied Microbiology*, 90(4), 489–493.
- Skaff, O., Pattison, D.I. & Davies, M.J. (2009) Hypothiocyanous acid reactivity with low-molecular-mass and protein thiols: absolute rate constants and assessment of biological relevance. *The Biochemical Journal*, 422(1), 111–117.
- Stulke, J., Hanschke, R. & Hecker, M. (1993) Temporal activation of beta-glucanase synthesis in *Bacillus subtilis* is mediated by the GTP pool. *Journal of General Microbiology*, 139(9), 2041–2045.
- Tenover, F.C., McDougal, L.K., Goering, R.V., Killgore, G., Projan, S.J., Patel, J.B. et al. (2006) Characterization of a strain of community-associated methicillin-resistant *Staphylococcus aureus* widely disseminated in the United States. *Journal of Clinical Microbiology*, 44(1), 108–118.
- Thomas, E.L. & Aune, T.M. (1978) Lactoperoxidase, peroxide, thiocyanate antimicrobial system: correlation of sulfhydryl oxidation with antimicrobial action. *Infection and Immunity*, 20(2), 456–463.
- Van Loi, V., Busche, T., Fritsch, V.N., Weise, C., Gruhlke, M.C.H., Slusarenko, A.J. et al. (2021) The two-Cys-type TetR repressor GbaA confers resistance under disulfide and electrophile stress in *Staphylococcus aureus*. *Free Radical Biology & Medicine*, 177, 120–131.
- Vestergaard, M., Frees, D. & Ingmer, H. (2019) Antibiotic resistance and the MRSA problem. *Microbiology Spectrum*, 7(2). Available from: <https://doi.org/10.1128/microbiolspec.GPP3-0057-2018>
- van der Vliet, A. (2008) NADPH oxidases in lung biology and pathology: host defense enzymes, and more. *Free Radical Biology & Medicine*, 44(6), 938–955.
- Voyich, J.M., Braughton, K.R., Sturdevant, D.E., Whitney, A.R., Saïd-Salim, B., Porcella, S.F. et al. (2005) Insights into mechanisms used by *Staphylococcus aureus* to avoid destruction by human neutrophils. *Journal of Immunology*, 175(6), 3907–3919.
- Wetzstein, M., Völker, U., Dedio, J., Löbau, S., Zuber, U., Schiesswohl, M. et al. (1992) Cloning, sequencing, and molecular analysis of the dnaK locus from *Bacillus subtilis*. *Journal of Bacteriology*, 174(10), 3300–3310.
- Wijkstrom-Frei, C., el-Chemaly, S., Ali-Rachedi, R., Gerson, C., Cobas, M.A., Forteza, R. et al. (2003) Lactoperoxidase and human airway host defense. *American Journal of Respiratory Cell and Molecular Biology*, 29(2), 206–212.
- Winterbourn, C.C., Hampton, M.B., Livesey, J.H. & Kettle, A.J. (2006) Modeling the reactions of superoxide and myeloperoxidase in the neutrophil phagosome: implications for microbial killing. *The Journal of Biological Chemistry*, 281(52), 39860–39869.
- Zajac, M., Dreano, E., Edwards, A., Planelles, G. & Sermet-Gaudelus, I. (2021) Airway surface liquid pH regulation in airway epithelium current understandings and gaps in knowledge. *International Journal of Molecular Sciences*, 22(7), 3384.

SUPPORTING INFORMATION

Additional supporting information can be found online in the Supporting Information section at the end of this article.

How to cite this article: Shearer, H.L., Loi, V.V., Weiland, P., Bange, G., Altegoer, F., Hampton, M.B., Antelmann, H. & Dickerhof, N. (2023). MerA functions as a hypothiocyanous acid reductase and defense mechanism in *Staphylococcus aureus*. *Molecular Microbiology*, 119, 456–470. <https://doi.org/10.1111/mmi.15035>